

7-25-2018

Exclusive Photoproduction of π Degrees up to Large Values of Mandelstam Variables s , t , and u with CLAS

M. C. Kunkel

M. J. Amarian

I. I. Strakovsky

J. Ritman

G. R. Goldstein

See next page for additional authors

Follow this and additional works at: <https://scholarship.richmond.edu/physics-faculty-publications>

Part of the [Physics Commons](#)

Recommended Citation

Kunkel, M. C., M. J. Amarian, I. I. Strakovsky, J. Ritman, G. R. Goldstein, K. P. Adhikari, S. Adhikari, G. Gilfoyle, et al. "Exclusive Photoproduction of π Degrees up to Large Values of Mandelstam Variables s , t , and u with CLAS." *Physical Review C* 98, no. 1 (July 25, 2018): 015207. <https://doi.org/10.1103/PhysRevC.98.015207>.

This Article is brought to you for free and open access by the Physics at UR Scholarship Repository. It has been accepted for inclusion in Physics Faculty Publications by an authorized administrator of UR Scholarship Repository. For more information, please contact scholarshiprepository@richmond.edu.

Authors

M. C. Kunkel, M. J. Amaryan, I. I. Strakovsky, J. Ritman, G. R. Goldstein, K. P. Adhikari, S. Adhikari, Gerard P. Gilfoyle, and et. al.

Exclusive photoproduction of π^0 up to large values of Mandelstam variables s , t , and u with CLAS

M. C. Kunkel,^{32,18} M. J. Amarian,^{32,*} I. I. Strakovsky,¹⁶ J. Ritman,^{3,18} G. R. Goldstein,⁴³ K. P. Adhikari,²⁸ S. Adhikari,¹³ H. Avakian,³⁹ J. Ball,⁷ I. Balossino,¹⁹ L. Barion,¹⁹ M. Battaglieri,²¹ V. Batourine,^{39,27} I. Bedlinskiy,²⁵ A. S. Biselli,^{11,5} S. Boiarinov,³⁹ W. J. Briscoe,¹⁶ W. K. Brooks,^{40,39} S. Bültmann,³² V. D. Burkert,³⁹ F. Cao,⁹ D. S. Carman,³⁹ A. Celentano,²¹ G. Charles,³² T. Chetry,³¹ G. Ciullo,^{19,12} L. Clark,⁴² P. L. Cole,¹⁷ M. Contalbrigo,¹⁹ O. Cortes,¹⁷ V. Crede,¹⁴ A. D'Angelo,^{22,35} N. Dashyan,⁴⁷ R. De Vita,²¹ E. De Sanctis,²⁰ P. V. Degtyarenko,³⁹ M. Defurne,⁷ A. Deur,³⁹ C. Djalali,³⁷ M. Dugger,² R. Dupre,²⁴ H. Egiyan,³⁹ A. El Alaoui,⁴⁰ L. El Fassi,²⁸ L. Elouadrhiri,³⁹ P. Eugenio,¹⁴ G. Fedotov,³¹ R. Fersch,^{8,46} A. Filippi,²³ A. Fradi,²⁴ G. Gavalian,^{39,29} Y. Ghandilyan,⁴⁷ S. Ghosh,¹⁰ G. P. Gilfoyle,³⁴ K. L. Giovanetti,²⁶ F. X. Girod,³⁹ D. I. Glazier,⁴² W. Gohn,^{9,†} E. Golovatch,³⁶ R. W. Gothe,³⁷ K. A. Griffioen,⁴⁶ L. Guo,^{13,39} M. Guidal,²⁴ K. Hafidi,¹ H. Hakobyan,^{40,47} N. Harrison,³⁹ M. Hattawy,¹ K. Hicks,³¹ M. Holtrop,²⁹ C. E. Hyde,³² D. G. Ireland,⁴² B. S. Ishkhanov,³⁶ E. L. Isupov,³⁶ D. Jenkins,⁴⁴ K. Joo,⁹ M. L. Kabir,²⁸ D. Keller,⁴⁵ G. Khachatryan,⁴⁷ M. Khachatryan,³² M. Khandaker,^{30,‡} A. Kim,⁹ W. Kim,²⁷ A. Klein,³² F. Klein,^{6,16} V. Kubarovsky,³⁹ S. E. Kuhn,³² J. M. Laget,^{39,7} L. Lanza,^{22,35} P. Lenisa,¹⁹ D. Lersch,¹⁸ K. Livingston,⁴² I. J. D. MacGregor,⁴² N. Markov,⁹ G. Mbianda Njencheu,³² B. McKinnon,⁴² T. Mineeva,^{40,9} V. Mokeev,^{39,36} R. A. Montgomery,⁴² A. Movsisyan,¹⁹ C. Munoz Camacho,²⁴ P. Nadel-Turonski,³⁹ S. Niccolai,²⁴ G. Niculescu,²⁶ M. Osipenko,²¹ A. I. Ostrovidov,¹⁴ M. Paolone,³⁸ K. Park,^{39,37} E. Pasyuk,³⁹ D. Payette,³² W. Phelps,^{13,16} O. Pogorelko,²⁵ J. Poudel,³² J. W. Price,⁴ S. Procureur,⁷ Y. Prok,^{32,45} D. Protopopescu,⁴² M. Ripani,²¹ B. G. Ritchie,² A. Rizzo,^{22,35} G. Rosner,⁴² A. Roy,¹⁰ F. Sabatié,⁷ C. Salgado,³⁰ S. Schadmand,¹⁸ R. A. Schumacher,⁵ Y. G. Sharabian,³⁹ Iu. Skorodumina,^{37,36} S. Stepanyan,³⁹ D. G. Ireland,⁴² D. Sokhan,⁴² D. I. Sober,⁶ N. Sparveris,³⁸ S. Strauch,^{37,16} M. Taiuti,^{21,15} J. A. Tan,²⁷ M. Ungaro,^{39,33} H. Voskanyan,⁴⁷ E. Voutier,²⁴ D. P. Watts,⁴¹ L. Weinstein,³² X. Wei,³⁹ D. P. Weygand,⁸ N. Zachariou,⁴¹ J. Zhang,⁴⁵ and Z. W. Zhao³²

(CLAS Collaboration)

¹Argonne National Laboratory, Argonne, Illinois 60439, USA

²Arizona State University, Tempe, Arizona 85287, USA

³Institut für Experimentalphysik I, Ruhr-Universität Bochum, 44780 Bochum, Germany

⁴California State University, Dominguez Hills, Carson, California 90747, USA

⁵Carnegie Mellon University, Pittsburgh, Pennsylvania 15213, USA

⁶The Catholic University of America, Washington, District of Columbia, 20064, USA

⁷IRFU, CEA, Université Paris-Saclay, F-91191 Gif-sur-Yvette, France

⁸Christopher Newport University, Newport News, Virginia 23606, USA

⁹University of Connecticut, Storrs, Connecticut 06269, USA

¹⁰Indian Institute of Technology, Simrol, Indore 453552, Madhya Pradesh, India

¹¹Fairfield University, Fairfield, Connecticut 06824, USA

¹²Università di Ferrara, 44121 Ferrara, Italy

¹³Florida International University, Miami, Florida 33199, USA

¹⁴Florida State University, Tallahassee, Florida 32306, USA

¹⁵Università di Genova, 16146 Genova, Italy

¹⁶The George Washington University, Washington, District of Columbia 20052, USA

¹⁷Idaho State University, Pocatello, Idaho 83209, USA

¹⁸Institut für Kernphysik, Forschungszentrum Jülich, 52424 Jülich, Germany

¹⁹INFN, Sezione di Ferrara, 44100 Ferrara, Italy

²⁰INFN, Laboratori Nazionali di Frascati, 00044 Frascati, Italy

²¹INFN, Sezione di Genova, 16146 Genova, Italy

²²INFN, Sezione di Roma Tor Vergata, 00133 Rome, Italy

²³INFN, Sezione di Torino, 10125 Torino, Italy

²⁴Institut de Physique Nucléaire, CNRS/IN2P3 and Université Paris Sud, Orsay, France

²⁵Institute of Theoretical and Experimental Physics, Moscow 117259, Russia

²⁶James Madison University, Harrisonburg, Virginia 22807, USA

²⁷Kyungpook National University, Daegu 41566, Republic of Korea

²⁸Mississippi State University, Mississippi State, Mississippi 39762-5167, USA

²⁹University of New Hampshire, Durham, New Hampshire 03824-3568, USA

³⁰Norfolk State University, Norfolk, Virginia 23504, USA

³¹Ohio University, Athens, Ohio 45701, USA

³²Old Dominion University, Norfolk, Virginia 23529, USA

³³Rensselaer Polytechnic Institute, Troy, New York 12180-3590, USA

³⁴University of Richmond, Richmond, Virginia 23173, USA

³⁵*Universita' di Roma Tor Vergata, 00133 Rome, Italy*³⁶*Skobeltsyn Institute of Nuclear Physics, Lomonosov Moscow State University, 119234 Moscow, Russia*³⁷*University of South Carolina, Columbia, South Carolina 29208, USA*³⁸*Temple University, Philadelphia, Pennsylvania 19122, USA*³⁹*Thomas Jefferson National Accelerator Facility, Newport News, Virginia 23606, USA*⁴⁰*Universidad Técnica Federico Santa María, Casilla 110-V Valparaíso, Chile*⁴¹*Edinburgh University, Edinburgh EH9 3JZ, United Kingdom*⁴²*University of Glasgow, Glasgow G12 8QQ, United Kingdom*⁴³*Tufts University, Medford, Massachusetts 02155, USA*⁴⁴*Virginia Polytechnic Institute and State University, Virginia 24061-0435, USA*⁴⁵*University of Virginia, Charlottesville, Virginia 22901, USA*⁴⁶*College of William and Mary, Williamsburg, Virginia 23187-8795, USA*⁴⁷*Yerevan Physics Institute, 375036 Yerevan, Armenia*

(Received 1 January 2018; revised manuscript received 5 February 2018; published 25 July 2018)

Exclusive photoproduction cross sections have been measured for the process $\gamma p \rightarrow p\pi^0[e^+e^-(\gamma)]$ with the Dalitz decay final state using tagged photon energies in the range of $E_\gamma = 1.275\text{--}5.425$ GeV. The complete angular distribution of the final state π^0 , for the entire photon energy range up to large values of t and u , has been measured for the first time. The data obtained show that the cross section $d\sigma/dt$, at mid to large angles, decreases with energy as $s^{-6.89 \pm 0.26}$. This is in agreement with the perturbative QCD quark counting rule prediction of s^{-7} . Paradoxically, the size of angular distribution of measured cross sections is greatly underestimated by the QCD-based generalized parton distribution mechanism at highest available invariant energy $s = 11$ GeV². At the same time, the Regge-exchange-based models for π^0 photoproduction are more consistent with experimental data.

DOI: [10.1103/PhysRevC.98.015207](https://doi.org/10.1103/PhysRevC.98.015207)

I. INTRODUCTION

In general, there are properties of π^0 that make this particle very special for our understanding of quantum chromodynamics (QCD). To name a few: it is the lightest element of all visible hadronic matter in the universe; according to its $q\bar{q}$ content the π^0 has a mass much less than one would expect from a constituent quark mass, $m \approx 350$ MeV; and it has an extremely short life time, $\tau \approx 10^{-16}$ s. Its main decay mode, $\pi^0 \rightarrow \gamma\gamma$, with a branching ratio $\approx 99\%$, played a crucial role in confirming the number of colors in QCD and in establishing the chiral anomaly in gauge theories. With all this being said, the structure and properties of π^0 are not completely understood.

One of the cleanest ways to obtain additional experimental information about the π^0 is high-energy photoproduction on a proton, as the incoming electromagnetic wave is structureless, contrary to any hadronic probe. Even after decades of

experimental efforts, precise data of the elementary reaction $\gamma p \rightarrow p\pi^0$, above the resonance region and at large values of all Mandelstam variables s , t , and u , are lacking.

At the interface between the crowded low-energy resonance production regime and the smooth higher-energy, small angle behavior, traditionally described by Regge poles [1], lies a region in which hadronic duality interpolates the excitation function between these regimes. Exclusive π photoproduction and π nucleon elastic scattering show this duality in a semilocal sense through finite energy sum rules (FESRs) [2]. The connection to QCD is more tenuous for on-shell photoproduction of pions at small scattering angles, but the quark content can become manifest through large fixed-angle dimensional counting rules [3,4], as well as being evident in semi-inclusive or exclusive electroproduction of pions, described through transverse momentum distributions (TMDs) and generalized parton distributions (GPDs).

The Regge pole description of photoproduction amplitudes has a long and varied history. For π^0 and η photoproduction, all applications rely on a set of known meson Regge poles. There are two allowed t -channel J^{PC} quantum numbers, the odd signature (odd spin) 1^{--} (ρ^0 , ω) and the 1^{+-} (b_1^0 , h_1) Reggeons. Regge cut amplitudes are incorporated into some models and are interpreted as rescattering of on-shell meson-nucleon amplitudes. The phases between the different poles and cuts can be critical in determining the polarizations and the constructive or destructive interferences that can appear. Four distinct Regge models are considered here.

An early model developed by Goldstein and Owens [5] has the exchange of leading Regge trajectories with appropriate

*Corresponding author: mamaryan@odu.edu

[†]Present address: University of Kentucky, Lexington, Kentucky 40506, USA.

[‡]Present address: Idaho State University, Pocatello, Idaho 83209, USA.

Published by the American Physical Society under the terms of the [Creative Commons Attribution 4.0 International](https://creativecommons.org/licenses/by/4.0/) license. Further distribution of this work must maintain attribution to the author(s) and the published article's title, journal citation, and DOI. Funded by SCOAP³.

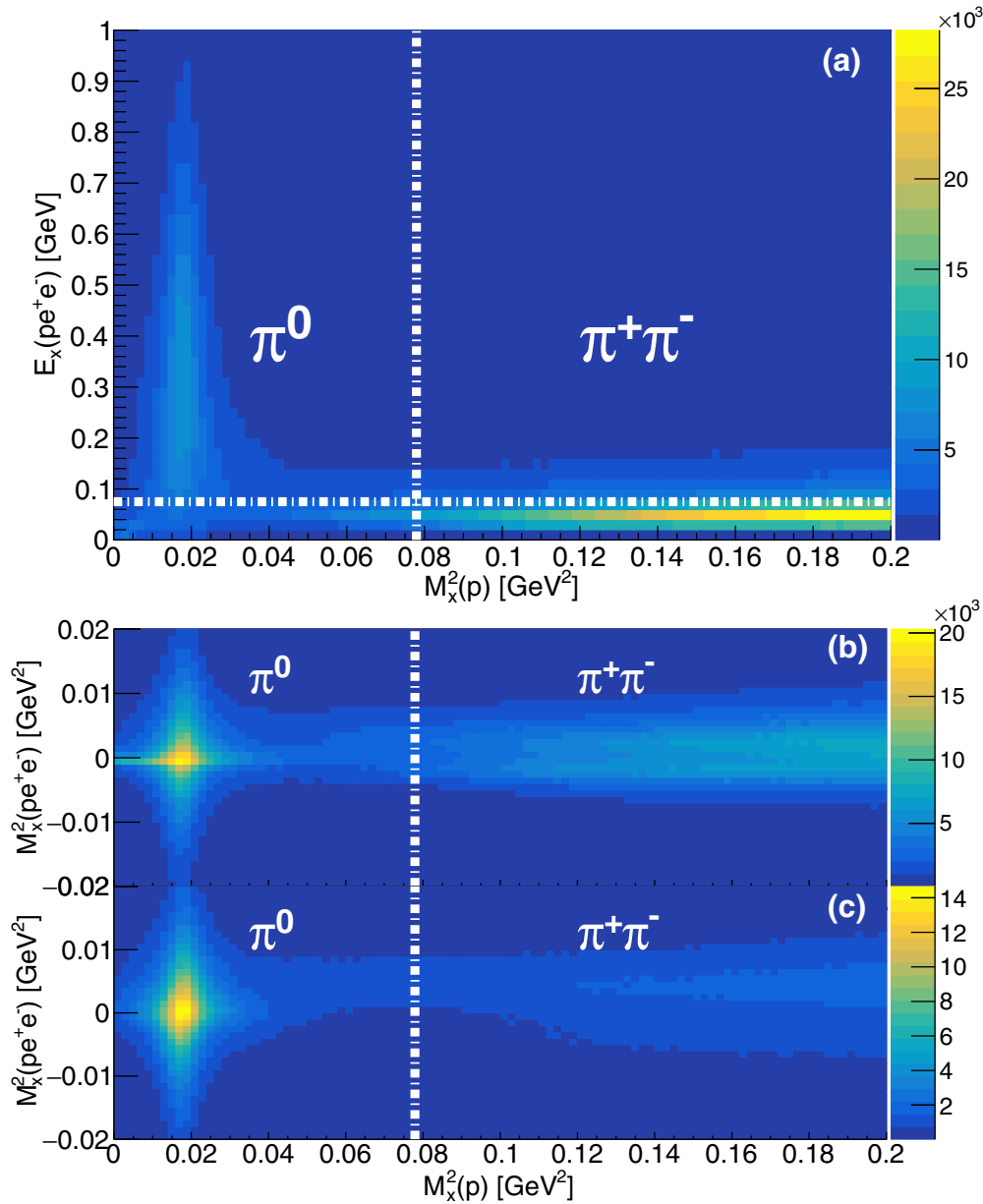


FIG. 1. (Top) (a) Missing energy $E_X(pe^+e^-)$ of all detected particles vs missing mass squared of the proton $M_X^2(p)$. (Bottom) Missing mass squared of all detected particles $M_X^2(pe^+e^-)$ vs missing mass squared of the proton $M_X^2(p)$: (b) before applying the the cut on missing energy, $E_X(pe^+e^-)$, (lower-top panel), and (c) after applying the cut $E_X(pe^+e^-) > 75$ MeV (lower-bottom panel). The horizontal white dashed-dotted line illustrates the 75 MeV threshold used in this analysis. The vertical white dashed-dotted line depicts the kinematic threshold for $\pi^+\pi^-$ production.

t -channel quantum numbers along with Regge cuts generated via final-state rescattering through Pomeron exchange. The Regge couplings to the nucleon were fixed by reference to electromagnetic form factors, $SU(3)_{\text{flavor}}$, and low-energy nucleon-nucleon meson exchange potentials. At the time, the range of applicability was taken to be above the resonance region and $|t| \leq 1.2 \text{ GeV}^2$, where t is the squared four-momentum transfer. Here we will let the t range extend to large values of t in order to see the predicted cross-section dips from the zeros in the Regge residues. Because even signature partners (A_2 , f_2) of the odd spin poles (ρ , ω) lie on the same trajectories, the Regge residues are required to have zeros to

cancel the even (wrong) signature poles in the physical region; these extra zeros are called nonsense wrong signature zeros (NWSZs) [6]. While the dip near $t \approx -0.5 \text{ GeV}^2$ is present in the π^0 cross-section data, it is absent in the beam asymmetry, Σ , measurement for π^0 and η photoproduction [7]. This is not explained by the standard form of the NWSZ Regge residues.

Quite recently, Mathieu *et al.* [8] (see also Ref. [9]), used the same set of Regge poles, but a simplified form of only ω -Pomeron cuts. They show that daughter trajectories are not significant as an alternative to the Regge cuts. However, to reproduce the absence of a dip in η photoproduction at $t \approx -0.5 \text{ GeV}^2$ they remove the standard wrong signature

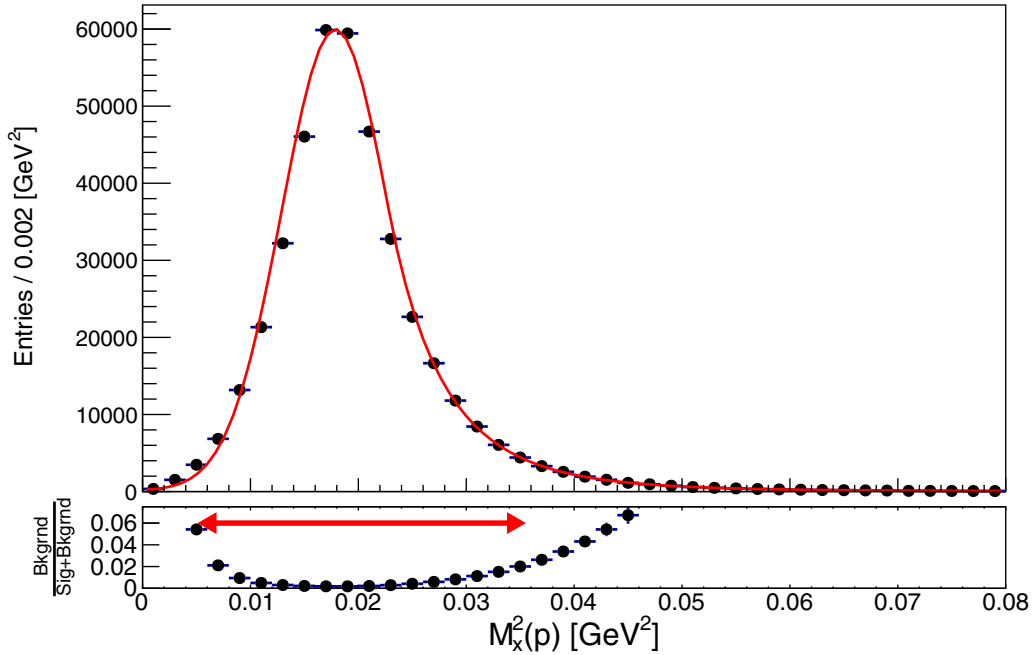


FIG. 2. (Top) Peak of π^0 in the proton missing mass squared distribution for events with $pe^+e^-(\gamma)$ in the final state with missing energy cut $E_x > 75$ MeV. The red solid line depicts the fit function (signal+background). (Bottom) Relative contributions of background. The red arrow indicates the range of the $M_x^2(p)$ distribution used to select π^0 events.

zero, i.e., the NWSZ. Donnachie and Kalashnikova [10] have included t -channel ρ^0 , ω , and b_1^0 exchange, but not the h_1 Reggeon, all with different parametrizations from Ref. [5]. They include ω , $\rho \otimes$ Pomeron cuts, as well as ω , $\rho \otimes f_2$ lower-lying cuts, which help to fill in the wrong signature zeros of the ω , ρ Regge pole residues. The model of Laget and collaborators [11] included u -channel baryon exchange, which dominate at backward angles, along with elastic and inelastic unitarity cuts to fill the intermediate t range.

With these ingredients, the model is expected to describe the full angular range ($\theta_\pi = 0 \rightarrow 180^\circ$), where θ_π is the pion polar angle in the cm frame, while the other models are good for more limited ranges of t [5,8,10]. Here, we examine how Regge phenomenology works for the energy range of $2.8 \text{ GeV} < E_\gamma < 5.5 \text{ GeV}$.

In addition to Regge pole models, the introduction of the handbag mechanism, developed by Kroll *et al.* [12], has provided complementary possibilities for the interpretation of hard exclusive reactions. In this approach, the reaction is factorized into two parts, one quark from the incoming and one from the outgoing nucleon participate in the hard sub-process, which is calculable using perturbative quantum chromodynamics (pQCD). The soft part consists of all the other partons that are spectators and can be described in terms of GPDs [13]. The handbag model applicability requires a hard scale, which, for meson photoproduction, is only provided by large transverse momentum, which corresponds to large angle production, roughly for $-0.6 \leq \cos \theta_\pi \leq 0.6$. Here, we examined how the handbag model may extend to the $\gamma p \rightarrow p\pi^0$ case proposed in Ref. [12]. The distribution amplitude for the quark+antiquark to π^0 is fixed by other phenomenology

and leads to the strong suppression of the production cross section.

Binary reactions in QCD with large momentum transfer occur via gluon and quark exchanges between the colliding particles. The constituent counting rules [3,4] provide a simple recipe to predict the energy dependence of the differential cross sections of two-body reactions at large angles when the ratio t/s is finite and is kept constant. The lightest meson photoproduction was examined in terms of these counting rules [14–18]. As was first observed at SLAC by Anderson *et al.* [14], the reaction $\gamma p \rightarrow n\pi^+$ shows agreement with constituent counting rules that predict the cross section should vary as s^{-7} . The agreement extends down to $s = 6 \text{ GeV}^2$ where the contribution of baryon resonances are still sizable. Here, we examined how applicable the counting rule is for $\gamma p \rightarrow p\pi^0$ up to $s = 11 \text{ GeV}^2$.

Earlier, untagged bremsstrahlung, measurements of $\gamma p \rightarrow p\pi^0$, for $2 \leq E_\gamma \leq 18 \text{ GeV}$ (1964–1979) provided 451 data points for differential cross section $d\sigma/dt$ [19], have very large systematic uncertainties and do not have sufficient accuracy to perform comprehensive phenomenological analyses. A previous CLAS measurement of $\gamma p \rightarrow p\pi^0$, for $2.0 \leq E_\gamma \leq 2.9 \text{ GeV}$, has an overall systematic uncertainty of 5% but only provided 164 data points for differential cross section $d\sigma/dt$ [20].

The results described here are the first to allow a detailed analysis, bridging the nucleon resonance and high-energy regions over a wide angular range, of exclusive pion photoproduction. By significantly extending the database they facilitate the examination of the resonance, Regge, and wide angle QCD regimes of phenomenology. The broad range of c.m. energy, \sqrt{s} , is particularly helpful in sorting out the phenomenology

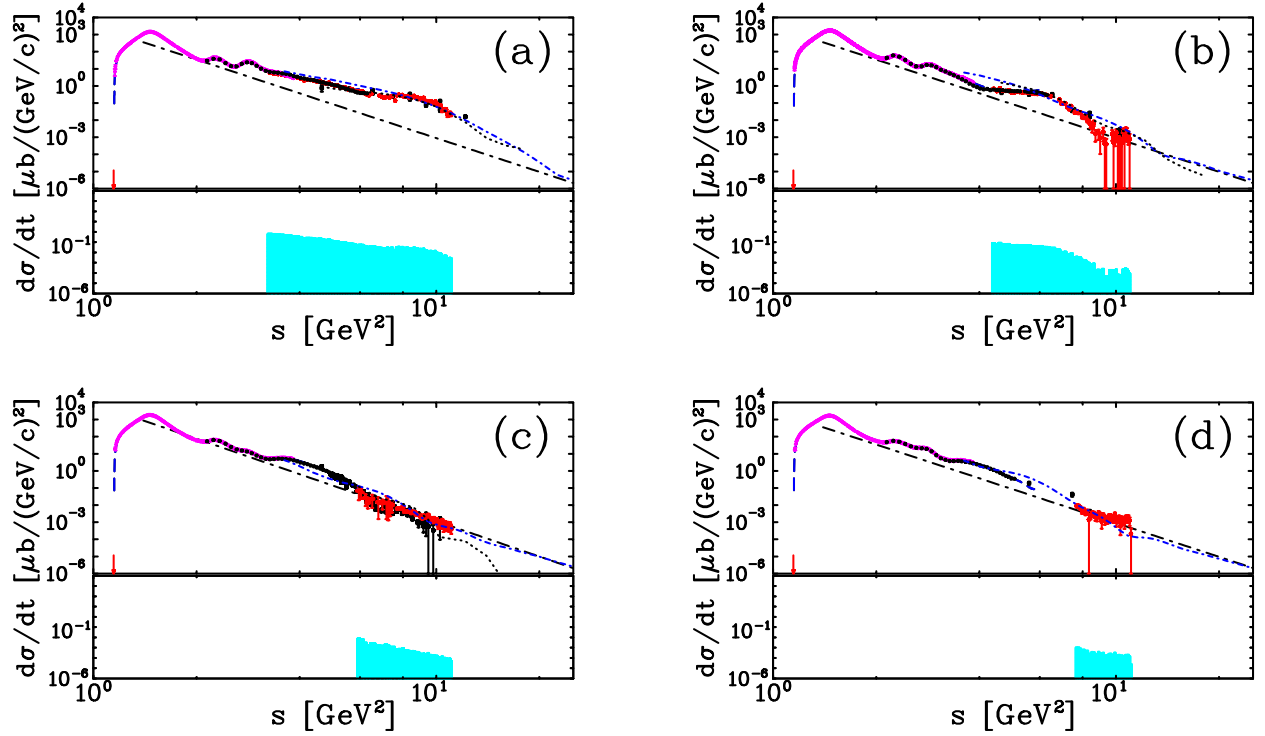


FIG. 3. Differential cross section $d\sigma/dt$ of the reaction $\gamma p \rightarrow p\pi^0$ at polar angles of (a) 50° , (b) 70° , (c) 90° , and (d) 110° in the c.m. frame as a function of c.m. energy squared, s . The red (solid circles) are the current g12 CLAS data. The recent tagged photon data are from [20] (black open circles) and [29] (magenta open diamonds with crosses starting from a threshold). The black solid squares are data from old bremsstrahlung measurements [19]. The plotted uncertainties are statistical. The systematic uncertainties are presented as a shaded area in the subpanel for each plot. The blue dashed line corresponds to the SAID PWA PR15 solution (no new CLAS g12 data are used for the fit) [29]. The black dot-dashed lines are plotted as the best-fit result of the power function s^{-n} , with $n = 6.89 \pm 0.26$, for the spectrum at 90° . The pion production threshold is shown as a vertical red arrow. The Regge results [5,11] are given by the black dotted line and the blue short dash-dotted line, respectively.

associated with both Regge and QCD-based models of the nucleon [21].

In this work, we provide a large set of differential cross section values for laboratory frame photon energies $E_\gamma = 1.25$ – 5.55 GeV, corresponding to a range of c.m. energies, $W = 1.81$ – 3.33 GeV. We have compared the Regge pole, the handbag, and the constituent counting rule phenomenology with the new CLAS experimental information on $d\sigma/dt$ for the $\gamma p \rightarrow p\pi^0$ reaction above the resonance regime. As will be seen, this data set quadruples the world database for π^0 photoproduction above $E_\gamma = 2$ GeV and together with the previous CLAS measurement [20] constrains the high-energy phenomenology well.

II. EXPERIMENT

The experiment was performed with the CLAS detector at Jefferson Laboratory [22] using a energy-tagged photon beam produced by bremsstrahlung from a 5.72 GeV electron beam, impinging upon a liquid hydrogen target, and was designated with the name g12. The experimental details are given in Ref. [23]. The reaction of interest is the photoproduction of neutral pions on a hydrogen target $\gamma p \rightarrow p\pi^0$, where the neutral pions decay into an $e^+e^-\gamma$ final state either due to external conversion, $\pi^0 \rightarrow \gamma\gamma \rightarrow e^+e^-\gamma$ or via Dalitz

decay $\pi^0 \rightarrow \gamma^*\gamma \rightarrow e^+e^-\gamma$. Requiring three charged tracks (p , e^+ , e^-) allowed the experiment to run at a much higher beam current than possible with single-prong detection, due to limitations of the trigger and data acquisition.

III. DATA ANALYSIS

Particle identification for the experiment was based on β vs. momentum times charge. Lepton identification was based on a kinematic constraint to the π^0 mass. Once the data was skimmed for p , π^+ , and π^- tracks, all particles that were π^+ , π^- were tentatively assigned to be electrons or positrons based on their charge (for details, see Refs. [24,25]). After particle selection, standard g12 calibration, fiducial cuts, and timing cuts were applied in the analysis [23].

Different kinematic fits were employed to cleanly identify the $\gamma p \rightarrow pe^+e^-(\gamma)$ reaction. They were applied to filter background from misidentified double-pion production to the single- π^0 production, to constrain the missing mass of entire final state to a missing photon and to ensure that the fit to the missing photon constrained the squared invariant mass of $e^+e^-(\gamma) = m_{\pi^0}^2$. The values of the confidence levels cuts employed was determined using the statistical significance to get the best signal-background ratio. The confidence levels for each constraint were

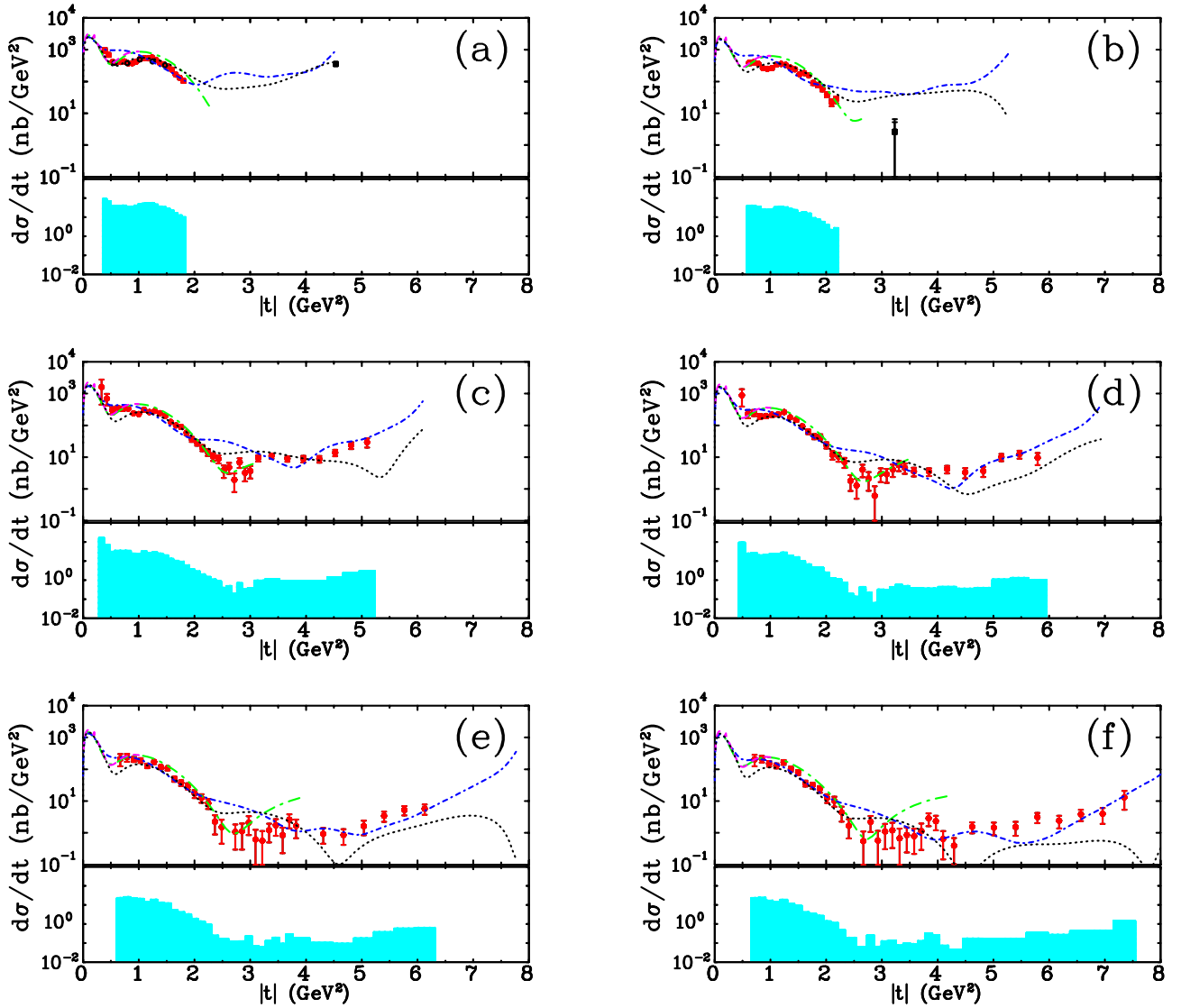


FIG. 4. Samples of the π^0 photoproduction cross section, $d\sigma/dt$, off the proton versus $|t|$ above the resonance regime: (a) $W = 2490$ MeV, (b) $W = 2635$ MeV, (c) $W = 2790$ MeV, (d) $W = 2940$ MeV, (e) $W = 3080$ MeV, and (f) $W = 3170$ MeV. The current data are indicated by red solid circles and a previous CLAS measurement [20] by black open circles. The black solid squares are from Ref. [19]. The plotted uncertainties are statistical. The systematic uncertainties are presented as a shaded area in the subpanel for each plot. Regge results [5,8,10,11] are given by black dotted line, green dot-dashed line, magenta long dashed line, and blue short dash-dotted line, respectively.

consistent between the g_{12} data and Monte Carlo simulations. Monte Carlo generation was performed using the PLUTO++ package [26].

The remainder of the background was attributed to $\pi^+\pi^-$ events. To reduce the background further, a comparison of the missing mass squared off the proton, $M_x^2(p) = (P_\gamma + P_p - P_p')^2$, in terms of the four-momenta of the incoming photon, target proton, and final-state proton, respectively, and the missing energy of detected system, $E_X(pe^+e^-) = E_\gamma + E_p - E_p' - E_{e^+} - E_{e^-}$, was performed, see Fig. 1. This comparison revealed that the majority of the $\pi^+\pi^-$ background has missing energy less than 75 MeV. To eliminate this background all events with a missing energy less than 75 MeV were removed.

The distribution of the proton missing mass squared for events with $pe^+e^-(\gamma)$ in the final state is shown in Fig. 2. A fit was performed with the crystal ball function [27,28] for the signal, plus a third-order polynomial function for the background. The total signal+background fit is shown by the red solid line. The fit resulted in $M_{\pi^0}^2 = 0.0179$ GeV² with a Gaussian width $\sigma = 0.0049$ GeV². To select π^0 events, an asymmetric cut about the measured value was placed in the range 0.0056 GeV² $\leq M_x^2(p) \leq 0.035$ GeV². This cut range can be seen as the arrow in the bottom panel of Fig. 2 along with the ratio of background events to the total number of events. As shown in Fig. 2, the event selection strategy for this analysis led to a negligible integrated background estimated to be no more than 1.05%.

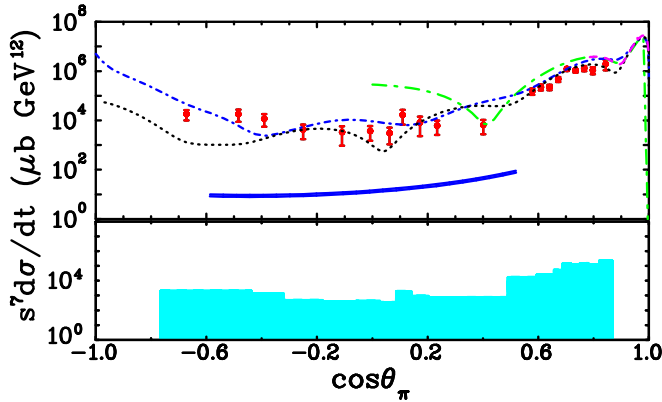


FIG. 5. Differential cross section of π^0 photoproduction. The CLAS experimental data at $s = 11 \text{ GeV}^2$ are from the current experiment (red solid circles). The plotted uncertainties are statistical. The systematic uncertainties are presented as a shaded area in the subpanel. The theoretical curves for the Regge fits are the same as in Fig. 4 and the Handbag model by Kroll *et al.* [12] (blue double solid line).

IV. RESULTS

As mentioned above there are two subprocesses that may lead to the same final state $\pi^0 \rightarrow e^+e^-\gamma$. Both subprocesses were simulated in the Monte Carlo with their corresponding branching ratios and used to obtain cross sections from experimentally observed yield of neutral pions.

The new CLAS high statistics $\gamma p \rightarrow p\pi^0$ cross sections from this analysis are compared in Figs. 3 and 4 with previous data [19,20,29]. The overall agreement is good, particularly with the previous CLAS data.

At higher energies (above $s \sim 6 \text{ GeV}^2$) and large c.m. angles ($\theta_\pi \geq 90^\circ$), the results are consistent with the s^{-7} scaling, at fixed t/s ratio, as expected from the constituent counting rule [3]. The black dash-dotted line at 90° (Fig. 3) is a result of the fit of new CLAS g_{12} data only, performed with a power function $\sim s^{-n}$, leading to $n = 6.89 \pm 0.26$. Structures observed at 50° and 70° up to $s \sim 11 \text{ GeV}^2$ indicate that the constituent counting rule requires higher energies and higher $|t|$ before it can provide a complete description. In Figs. 4 and 5, the $d\sigma/dt$ results are shown along with fits from Regge pole and cut [5,8,10,11] models and the handbag [12] model.

Figure 5 shows that the new CLAS data are orders of magnitude higher than the handbag model prediction by Kroll *et al.* [12] for π^0 photoproduction at $s = 11 \text{ GeV}^2$.

V. SYSTEMATIC UNCERTAINTIES

Systematic uncertainties in this experiment are stemming from different sources described below. One of them is due to the uncertainties related to the simulation of photon conversion and Dalitz branching ratio decay uncertainties, which total up to 1%. The target density and length uncertainty was estimated

to be on the order of 0.5%. Another source of the uncertainty is due to overall flux measurement and it was deduced to be on the order of 6%. Cut-based systematic uncertainty due to kinematic fit was on the order of 2%. The CLAS setup has a sixfold axial symmetry. The sector-to-sector uncertainties have been estimated to result in about (4.4–7.1)% depending on kinematics of our measurement. The overall systematic uncertainties of the experiment were below $\sim 12\%$ and are depicted as bands below the data in Figs. 3–5.

VI. CONCLUSIONS

In this experiment a novel approach was employed based on the π^0 Dalitz decay mode. Although this decay mode has a branching fraction of only about 1%, the enhanced event trigger selectivity enabled the figure of merit to be sufficiently high in order to extend the existing world measurements into an essentially unmeasured *terra incognita* domain. Through the experiments described above, an extensive and precise data set (2030 data points) on the differential cross section for π^0 photoproduction from the proton has been obtained for the first time, except for a few points from previous measurements, over the range of $1.81 \leq W \leq 3.33 \text{ GeV}$.

The measurements obtained here have been compared to existing data. The overall agreement is good, while the data provided here quadrupled the world bremsstrahlung database above $E_\gamma = 2 \text{ GeV}$ and covered the previous reported energies with finer resolution. This new and greatly expanded set of data provides strong confirmation of the basic features of models based on Regge poles and cuts. There is sufficient precision to discriminate among the distinct components of those models. Guided by these data, extensions of models and improved parametrizations are now possible.

From another perspective, the wide angle data agree with the pQCD-based constituent counting rules. Yet, a significant paradox now appears: the wide angle data disagree—by orders of magnitude—with a handbag model that combines pQCD with the soft region represented by GPDs. This is an important result that needs to be better understood.

ACKNOWLEDGMENTS

We thank Stanley Brodsky, Alexander Donnachie, Peter Kroll, Vincent Mathieu, and Anatoly Radyushkin for discussions of our measurements. We would like to acknowledge the outstanding efforts of the staff of the Accelerator and the Physics Divisions at Jefferson Lab that made the experiment possible. This work was supported in part by the Italian Istituto Nazionale di Fisica Nucleare, the French Centre National de la Recherche Scientifique and Commissariat à l’Energie Atomique, the United Kingdom’s Science and Technology Facilities Council (STFC), the US DOE and NSF, and the National Research Foundation of Korea. This material is based upon work supported by the U.S. Department of Energy, Office of Science, Office of Nuclear Physics, under Contract No. DE-AC05-06OR23177.

[1] J. P. Ader, M. Capdeville, and P. Salin, *Nucl. Phys. B* **3**, 407 (1967).

[2] H. K. Armenian, G. R. Goldstein, J. P. Rutherford, and D. L. Weaver, *Phys. Rev. D* **12**, 1278 (1975).

- [3] S. J. Brodsky and G. R. Farrar, *Phys. Rev. Lett.* **31**, 1153 (1973).
- [4] V. A. Matveev, R. M. Muradyan, and A. N. Tavkhelidze, *Lett. Nuovo Cim.* **5**, 907 (1972).
- [5] G. R. Goldstein and J. F. Owens, *Phys. Rev. D* **7**, 865 (1973).
- [6] C. B. Chiu, *Nucl. Phys. B* **30**, 477 (1971).
- [7] H. Al Ghouli *et al.* (GlueX Collaboration), *Phys. Rev. C* **95**, 042201 (2017).
- [8] V. Mathieu, G. Fox, and A. P. Szczepaniak, *Phys. Rev. D* **92**, 074013 (2015); J. Nys *et al.* (JPAC Collaboration), *ibid.* **95**, 034014 (2017).
- [9] V. L. Kashevarov, M. Ostrick, and L. Tiator, *Phys. Rev. C* **96**, 035207 (2017).
- [10] A. Donnachie and Y. S. Kalashnikova, *Phys. Rev. C* **93**, 025203 (2016).
- [11] J. M. Laget, *Phys. Lett. B* **695**, 199 (2011).
- [12] H. W. Huang and P. Kroll, *Eur. Phys. J. C* **17**, 423 (2000); H. W. Huang, R. Jakob, P. Kroll, and K. Passek-Kumericki, *ibid.* **33**, 91 (2004); M. Diehl and P. Kroll, *ibid.* **73**, 2397 (2013).
- [13] X. D. Ji, *Phys. Rev. D* **55**, 7114 (1997); A. V. Radyushkin, *Phys. Lett. B* **380**, 417 (1996); *Phys. Rev. D* **56**, 5524 (1997); D. Müller, D. Robaschik, B. Geyer, F.-M. Dittes, and J. Horejsi, *Fortsch. Phys.* **42**, 101 (1994).
- [14] R. L. Anderson, D. Gustavson, D. Ritson, G. A. Weitsch, H. J. Halpern, R. Prepost, D. H. Tompkins, and D. E. Wiser, *Phys. Rev. D* **14**, 679 (1976).
- [15] D. A. Jenkins and I. I. Strakovsky, *Phys. Rev. C* **52**, 3499 (1995).
- [16] L. Y. Zhu *et al.* (Jefferson Lab Hall A Collaboration), *Phys. Rev. Lett.* **91**, 022003 (2003).
- [17] W. Chen *et al.* (CLAS Collaboration), *Phys. Rev. Lett.* **103**, 012301 (2009).
- [18] K. J. Kong, T. K. Choi, and B. G. Yu, *Phys. Rev. C* **94**, 025202 (2016).
- [19] The Durham HEP Reaction Data Databases (UK) (Durham HepData), <http://durpdg.dur.ac.uk/hepdata/reac.html>.
- [20] M. Dugger *et al.* (CLAS Collaboration), *Phys. Rev. C* **76**, 025211 (2007).
- [21] P. Kroll, *Eur. Phys. J. A* **53**, 130 (2017), and references therein.
- [22] B. A. Mecking *et al.* (CLAS Collaboration), *Nucl. Instrum. Methods A* **503**, 513 (2003).
- [23] G12 Experimental Group, CLAS-NOTE 2017-002, 2017, <https://misportal.jlab.org/ul/Physics/Hall-B/clas/viewFile.cfm/2017-002?documentId=756>.
- [24] M. C. Kunkel, CLAS-NOTE 2017-005, 2017, <https://misportal.jlab.org/ul/Physics/Hall-B/clas/viewFile.cfm/2017-005?documentId=767>.
- [25] M. C. Kunkel, Ph. D. thesis, Old Dominion University, 2014, https://www.jlab.org/Hall-B/general/thesis/Kunkel_thesis.pdf.
- [26] I. Froehlich *et al.*, PoS ACAT2007, 076 (2007).
- [27] M. J. Oreglia, Ph. D. thesis, Stanford University, 1986, <https://search.proquest.com/docview/303036283>.
- [28] T. Skwarnicki, Ph. D. thesis, Institute of Nuclear Physics, Cracow, Poland, 1986, <http://inspirehep.net/record/230779/files/f31-86-02.pdf>.
- [29] P. Adlarson *et al.* (A2 Collaboration at MAMI), *Phys. Rev. C* **92**, 024617 (2015).